

Article

Novel Sulfamethoxazole Organotin Complexes: Synthesis, Characterization, and Hydrogen Storage Application

Dina S. Ahmed ¹, Noor Emad ², Mohammed Kadhom ³, Emad Yousif ^{2,*} and Mohammed Al-Mashhadani ²

¹ Department of Chemical Industries, Institute of Technology-Baghdad, Middle Technical University, 17564 Baghdad, Iraq; dina_saadi@mtu.edu.iq

² Department of Chemistry, College of Science, Al-Nahrain University, Baghdad 10072, Iraq; noor.emadf@ced.nahrainuniv.edu.iq (N.E.); mohammed.mashhadani@nahrainuniv.edu.iq (M.A.-M.)

³ Department of Environmental Science, College of Energy and Environmental Sciences, Alkarkh University of Science, Baghdad 10081, Iraq; kadhom@kus.edu.iq

* Correspondence: emad.yousif@nahrainuniv.edu.iq

Abstract: This study presents the synthesis and characterization of novel sulfamethoxazole organotin complexes and evaluates their potential for hydrogen storage applications. The synthesized complexes were characterized using various techniques, such as Nuclear Magnetic Resonance and Fourier Transform Infrared spectroscopy to determine their constructional and physicochemical properties. Field Emission Scanning Electron Microscopy was applied to analyze the surface morphology, and the Brunauer–Emmett–Teller method was utilized to measure the surface area. High-pressure adsorption experiments demonstrated the remarkable hydrogen storage capabilities of these complexes, with the highest hydrogen uptake of 29.1 cm³/g observed at 323 K. The results suggest that the prepared sulfamethoxazole organotin complexes have the potential to be candidates for gas separation and storage applications.

Keywords: sulfamethoxazole; tin complexes; gas separation; gas storage; gases uptake



Citation: Ahmed, D.S.; Emad, N.; Kadhom, M.; Yousif, E.; Al-Mashhadani, M. Novel Sulfamethoxazole Organotin Complexes: Synthesis, Characterization, and Hydrogen Storage Application. *Hydrogen* **2024**, *5*, 872–881. <https://doi.org/10.3390/hydrogen5040045>

Academic Editors: Mohamed Louzazni, Tariq Kamal and Emanuel Philippe Pereira Soares Ramos

Received: 30 July 2024

Revised: 1 November 2024

Accepted: 7 November 2024

Published: 13 November 2024



Copyright: © 2024 by the authors. Licensee MDPI, Basel, Switzerland. This article is an open access article distributed under the terms and conditions of the Creative Commons Attribution (CC BY) license (<https://creativecommons.org/licenses/by/4.0/>).

1. Introduction

Ongoing efforts persist in the quest for exceptionally efficient porous materials to alleviate the detrimental impacts of carbon dioxide on well-being and the natural surroundings. Carbon dioxide (CO₂) is a significant driver of global warming as it is one of the top greenhouse gases (GHGs) that evidentially contributes to raising the earth's temperatures, posing a threat to the long-term viability of life [1]. Fossil fuel production and combustion emit different GHGs, so finding an alternative source of energy has become crucial nowadays. As an illustration, fossil fuel power plants produce 85% of the global electrical supply and are substantial contributors to CO₂ emissions. This has a significant impact on global climate change [2–5]. Hydrogen is considered one of the most environmentally friendly energy sources, generating only water as a byproduct when combusted [6]. As a result, advancing efficient and safe hydrogen storage methods is vital [7]. A conventional approach to storing hydrogen is through chemisorption, with much research centered on metal hydrides [8]. Alternatively, hydrogen can be stored via physisorption in porous materials like porous carbons, which offer advantages such as high stability and easy accessibility [9]. The temperature at which adsorption takes place mostly depends on two factors: the reaction potential and the design or structure of the adsorbents. Therefore, it is essential to conduct comprehensive physical and chemical studies to examine the bonding states and interactions of functional groups on the surface of the adsorbent [10].

Characterizing pore size distribution is crucial in the description of porous materials. In fact, porous materials possess pores of varying sizes and numbers, which can be categorized as either closed or open pores depending on their degree of openness. As per the classifications provided by the International Union of Pure and Applied Chemistry

(IUPAC), pores are classified as either closed or open based on their level of accessibility. However, porous materials are divided into three subgroups depending on the diameter of the pores (d): macroporous ($d > 50$ nm), mesoporous (2 nm $< d < 50$ nm), and microporous ($d < 2$ nm) [11]. Current studies focused on a range of porous substances, such as molecular sieves, activated carbon, ceramics, organic polymers (such as the metal–organic compounds (MOF) and covalent organic compounds (COF)), and other nanomaterials [12–18].

Significant progress has been made in exploring novel adsorbents for hydrogen capture, which has motivated our group to investigate heterocyclic compounds containing sulfamethoxazole. These compounds exhibit high biological activity [19], acting as antibiotics and containing two distinct aromatic rings with substantial quantities of nitrogen, oxygen, and sulfur [20,21]. We investigated the potential of enhancing H_2 adsorption by utilizing certain characteristics. To do this, we conducted a unique synthesis based on Schiff's laws and utilized this method to assess hydrogen capture.

This study investigates the utilization of sulfamethoxazole as a ligand for the synthesis of novel tin complexes, which were subsequently evaluated for their potential as hydrogen storage materials. Various methods were applied to test the physical, chemical, and morphological characteristics of the produced complexes. The results indicate that these materials exhibit potential for gas storage applications, offering a possible solution to concerns regarding gas pollution and global warming.

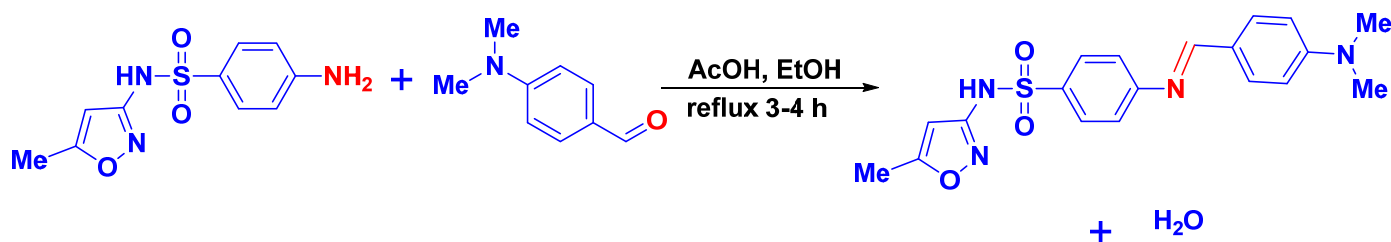
2. Experimental Setup

2.1. Instruments

FTIR spectra were obtained using a Bruker Fourier Transform Infrared (FTIR) spectrometer from Japan. The carbon, nitrogen, and hydrogen elemental analysis of the fabricated Schiff bases was performed utilizing a Vario EL III elemental analyzer made by Elementar Americas Inc., NY, USA. SEM pictures were acquired by applying a KYKY-EM3200 microscope working at an acceleration voltage of 25 kV. An elemental dispersive X-ray (EDX) examination was conducted on the complexes using a TESCAN MIRA3 LMU apparatus in Kohotovice, Czech Republic. The analysis was performed with an accelerating voltage of 15 kV. Proton nuclear magnetic resonance (1H -NMR) spectra were obtained employing a 400 MHz instrument, whereas tin-119 nuclear magnetic resonance (^{119}Sn -NMR) spectra were acquired employing a Bruker DRX300 NMR spectrometer (Bruker, Zürich, Switzerland) operating at 107 MHz. The substances were dissolved in deuterated dimethyl sulfoxide (DMSO- d_6). Nitrogen (N_2) adsorption and desorption isotherms were determined at a temperature of 77 K using a Quantachrome analyzer manufactured by Quantachrome Instruments in Boynton Beach, FL, USA. Prior to measurement, the samples were subjected to a drying process at a temperature of 120 °C in a vacuum oven (Cascade TEK, Cornelius, OR, USA) for a duration of 2 h, with a continuous flow of dry nitrogen gas. The specific surface area was estimated by applying the Brunauer–Emmett–Teller (BET) relationship at a relative pressure (P/P_0) of 0.98. In addition, the Barrett–Joyner–Halenda (BJH) method was applied to assess pore size distribution.

2.2. Fabrication of Sulfamethoxazole with Para Dimethyl Amino Benzaldehyde (L)

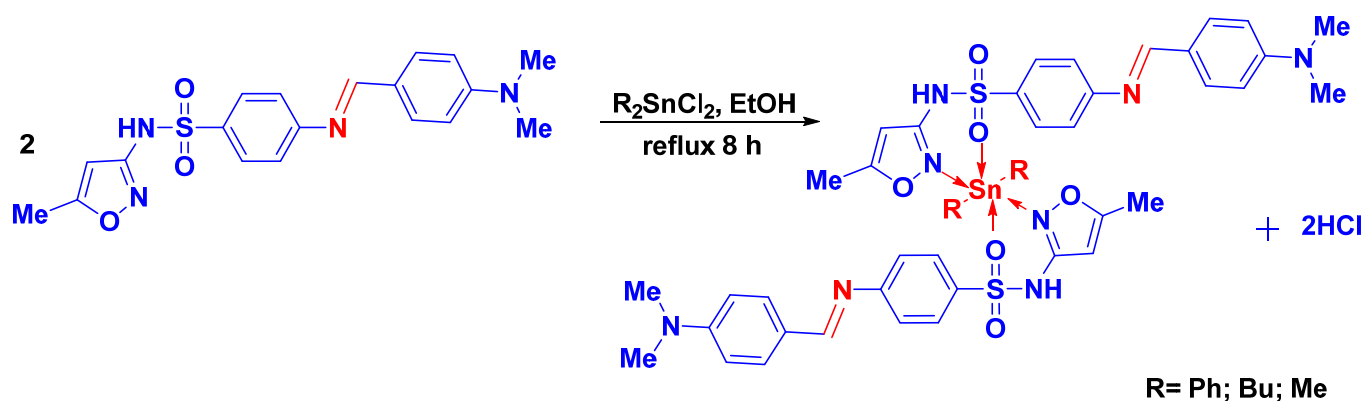
A mixture of 0.01 mole (1.49 g) of aldehyde (4-dimethylaminobenzaldehyde) was dissolved in 10 mL of absolute ethanol. Later, a few drops of glacial acetic acid were mixed with the solution. After 1 h, 0.01 mole (2.53 g) of sulfamethoxazole, dissolved in 10 mL of ethanol, was added to the mixture and refluxed for 3–4 h. The reaction was observed by TLC utilizing a hexane acetate (3:1) solvent system. After the reaction, the solution was allowed to cool down to ambient temperature, and the colored precipitate was filtered, rinsed with cold ethanol, and dried at an ambient temperature for 24 h. The resulting Schiff base is depicted in Scheme 1.



Scheme 1. Synthesis of sulfamethoxazole Schiff base.

2.3. Fabrication of Inorganic Complexes of Organotin Compounds with Ligand

Complexes were prepared using a molar ratio of 1:2 (organotin). Appropriate amounts of Ph_2SnCl_2 (3.438 g, 0.01 mol), Bu_2SnCl_2 (3.038 g, 0.01 mol), and Me_2SnCl_2 (2.197 g, 0.01 mol) were each dissolved in 5 mL of methanol. Following that, these solutions were added to a stirred solution of L (sulfamethoxazole with 4-dimethylaminobenzaldehyde) (5.06 g, 0.02 mol) in 5 mL of ethanol; this blend was refluxed for 8 h. The final solution was filtered, heated to dry, and recrystallized to form precipitates, as illustrated in Scheme 2. Furthermore, Table 1 shows the physical properties of the synthesized sulfamethoxazole tin complexes.



Scheme 2. Complexation of Schiff base with organotin.

Table 1. Physical properties of sulfamethoxazole tin complexes.

Compounds	Color	M.P. (°C)	Yield (%)
L	Yellowish orange	176–178	87
$[\text{Ph}_2\text{SnL}_2]$	Orange	167–169	84
$[\text{Bu}_2\text{SnL}_2]$	Auburn	156–158	81
$[\text{Me}_2\text{SnL}_2]$	Orange	144–146	75

3. Results and Discussion

3.1. FTIR Spectroscopy

Important data for functional groups were obtained from the FTIR analysis. For the Schiff base (L), the NH_2 bands at 3462 cm^{-1} and 3372 cm^{-1} disappeared, and the imine ($\text{C}=\text{N}$) band appeared at 1660 cm^{-1} . The asymmetric and symmetric $\text{S}=\text{O}$ bands were at 1363 cm^{-1} and 1151 cm^{-1} . After the reaction between the Schiff base and the three organotin compounds, many bands shifted, and new bands appeared, indicating the linkage between the O and N atoms with the Sn metal. All these changes are listed in Table 2.

Table 2. FTIR bands of Schiff base and sulfamethoxazole tin complexes.

Compound	NH ₂ Amine	ν (NH) Amid	ν (C=N) Schiff Base	ν (C=N) Lactam	ν (S=O) Asym.	ν (S=O) Sym.	ν (Sn- N)	ν (Sn-O)
Sulfamethoxazole	3462 3372	3295	-	1592	1359	1151	-	-
Schiff base (L)		3282	1660	1596	1363	1155	-	-
[Ph ₂ SnL ₂]		-	1645	1588	1368	1159	560	457
[Bu ₂ SnL ₂]		3282	1654	1585	1364	1156	524	-
[Me ₂ SnL ₂]		3293	1650	1583	1332	1155	552	467

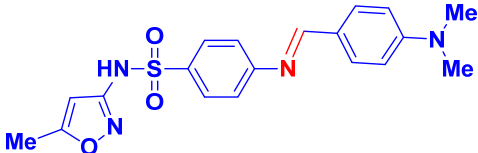
3.2. ¹H-NMR Spectra

The ¹H-NMR spectrum of the synthesized Schiff base (L) in DMSO-d₆ displayed a singlet at $\delta = 2.88$ ppm, which was assigned to the protons of the CH₃ group. The signal at a chemical shift of $\delta = 2.27$ ppm was attributed to the CH₃ protons of the isoxazole ring. The protons of the two aromatic benzene rings appeared as a multiplet in the range of $\delta = 6.63$ – 7.94 ppm. The proton of the CH=N group was observed as a singlet at $\delta = 8.87$ ppm [22,23]. Meanwhile, the NH proton was identified by a signal at $\delta = 10.36$ ppm, as shown in Figure S1 in the Supplementary File.

3.3. ¹³C-NMR Spectra

This analysis is used in chemistry to study carbon nuclei, aiding in determining the structures of unknown compounds and establishing a definitive formula. Carbon NMR offers direct insights into the structure of the synthesized compounds [24]. The detailed results are presented in Table 3 and Figure S2 in the Supplementary File.

Table 3. ¹³C-NMR data for Schiff base.

Compound	¹³ C-NMR (400 MHz): DMSO-d ₆ , δ , ppm in Hz)
	174.96, 166.33, 160.13, 156.02, 155.37, 136.14, 131.93, 130.42, 123.30, 118.69, 112.26, 99.80, 42.60, 13.65.

3.4. Characterization by (¹¹⁹Sn-NMR) Spectroscopy

Sn-NMR spectroscopy was employed to investigate the structural characteristics of organotin(IV) complexes [25,26]. The results, which depend on the chemical transformations influenced by the tin coordination number, revealed a single sharp peak, indicating the presence of a single type of tin species. The ¹¹⁹Sn-NMR spectra of the tin complexes were recorded in DMSO-d₆ solvent. The chemical shift data are presented in Table 4, with additional details provided in Figures S3–S5 in the Supplementary File.

Table 4. ¹¹⁹Sn-NMR spectra for sulfamethoxazole tin complexes.

Compound	δ ppm
Ph ₂ SnL ₂	−404.93
Bu ₂ SnL ₂	−215.01
Me ₂ SnL ₂	−242.53

3.5. FESEM Analysis

The morphology of the ligand and metal complexes was analyzed utilizing FESEM. The FESEM pictures, as illustrated, show a heterogeneous structure with good porosity of

various sizes and shapes, which is reliable for hydrogen gas storage. These characteristics are shown in Figure 1.

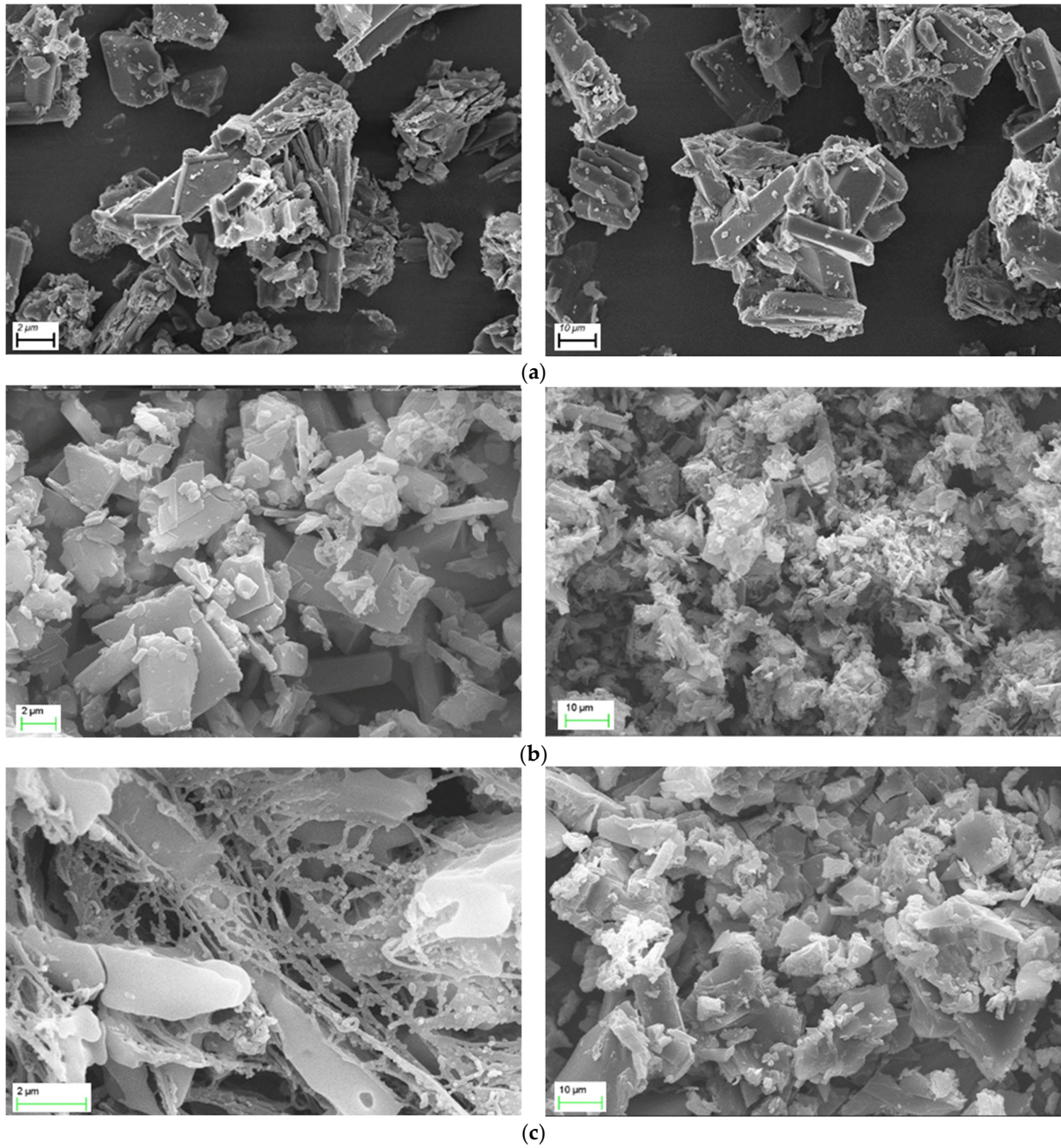
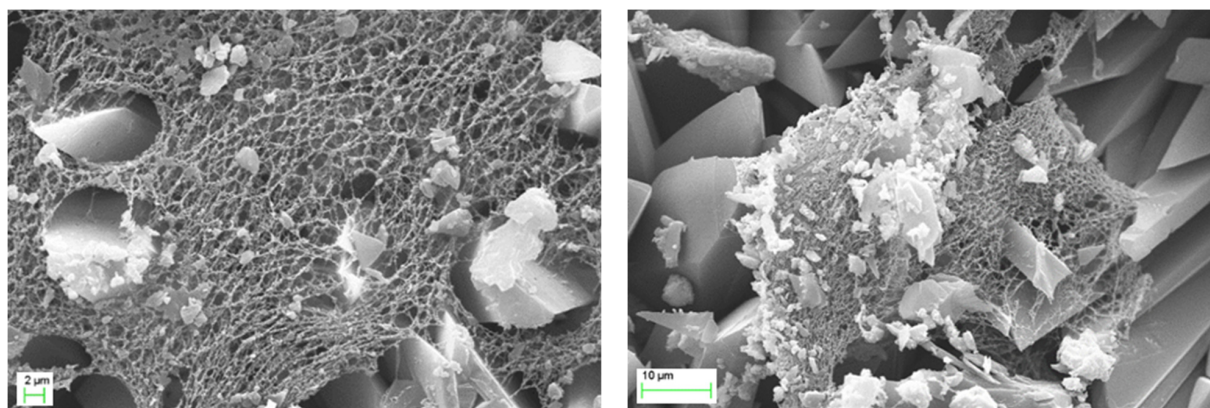


Figure 1. *Cont.*



(d)

Figure 1. SEM pictures of (a) sulfamethoxazole Schiff base (L), (b) Ph_2SnL_2 , (c) Bu_2SnL_2 , and (d) Me_2SnL_2 .

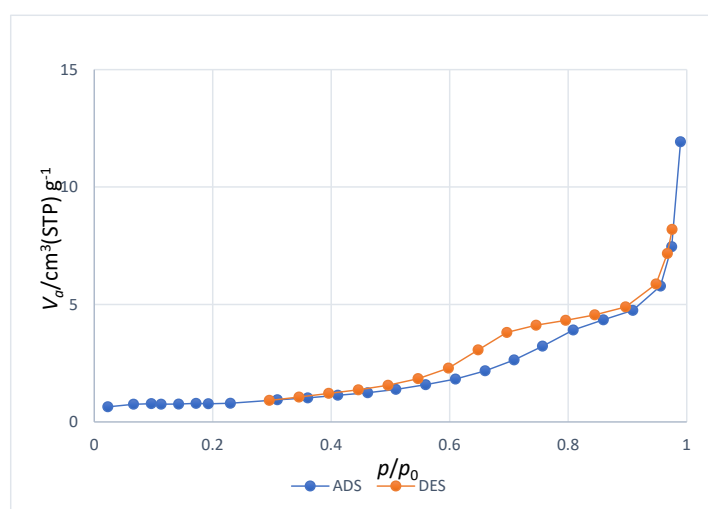
3.6. Measurements Nitrogen Adsorption of Metal Complex

The specific surface area was estimated by applying the Brunauer–Emmett–Teller (BET) method, which involved analyzing nitrogen (N_2) adsorption–desorption isotherms [27]. The adsorbents' porosity provides valuable information about their physicochemical interactions with the gas they absorb. The adsorption isotherm for sulfamethoxazole tin complexes is categorized as type III, suggesting that monolayer formation is absent.

The pore volume and BET surface area were determined by analyzing nitrogen adsorption–desorption isotherms at a relative pressure of 0.9. The BJH method was employed to compute the pore size and volume; the specific outcomes are given in Table 5. The pore volume and BET surface area were found using nitrogen adsorption, whereas the average pore diameter according to the BJH method was obtained from the desorption data provided in Figure 2a–c.

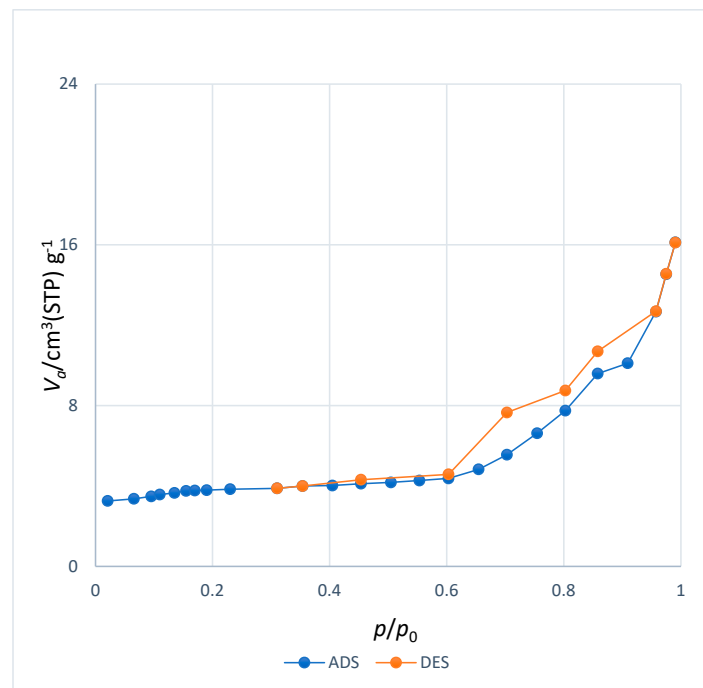
Table 5. Surface area, pore volume, and average pore diameter of sulfamethoxazole tin complexes.

Comp.	S_{BET} ($\text{m}^2 \cdot \text{g}^{-1}$)	Pore Volume ($\text{cm}^3 \cdot \text{g}^{-1}$)	Average Pore Diameter (nm)
Ph_2SnL_2	3.049 ± 0.42	0.018 ± 0.001	24.2 ± 2.71
Bu_2SnL_2	13.792 ± 1.89	0.026 ± 0.002	7.2 ± 0.99
Me_2SnL_2	5.5197 ± 0.84	0.024 ± 0.002	17.4 ± 2.46

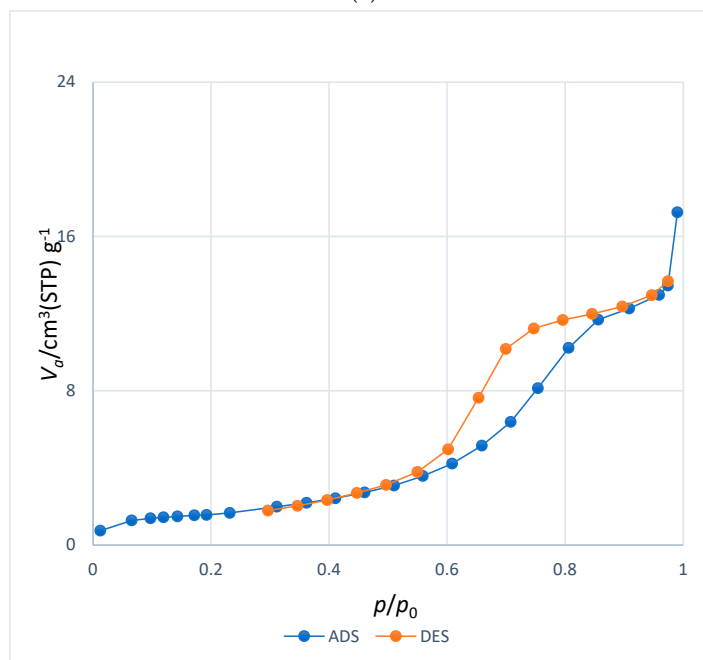


(a)

Figure 2. Cont.



(b)



(c)

Figure 2. N₂ adsorption (ADS) and desorption (DES) isotherms of sulfamethoxazole (a) di phenyl, (b) di butyl, and (c) di methyl tin complexes.

3.7. Hydrogen Uptake of Sulfamethoxazole Tin Complexes

The gas adsorption capacity of the fabricated complex was measured employing a high-pressure volumetric adsorption instrument, namely, the H-sorb 2600. The complex underwent degassing under vacuum and was subjected to heating at 100 °C for a duration of 1 h in order to remove any solvent or water that could be trapped within the pores. To ensure precision, the gas absorption test was again conducted using the same conditions to identify the ideal pressure. The factors that influence gas adsorption are the size of the pores, the charge of the metal, the kind of ligand, and the strength of the contact, like hydrogen bonds and Van der Waals forces, between the adsorbate and adsorbent [28,29]. Pore volume

is essential in assessing gas adsorption capacity, with larger pores enabling greater gas storage. Additionally, strong attractive forces, including electrostatic interactions and Van der Waals forces, noticeably enhance H₂ uptake [30–32]. Figure 3 illustrates the gas adsorption isotherms for sulfamethoxazole tin complexes.

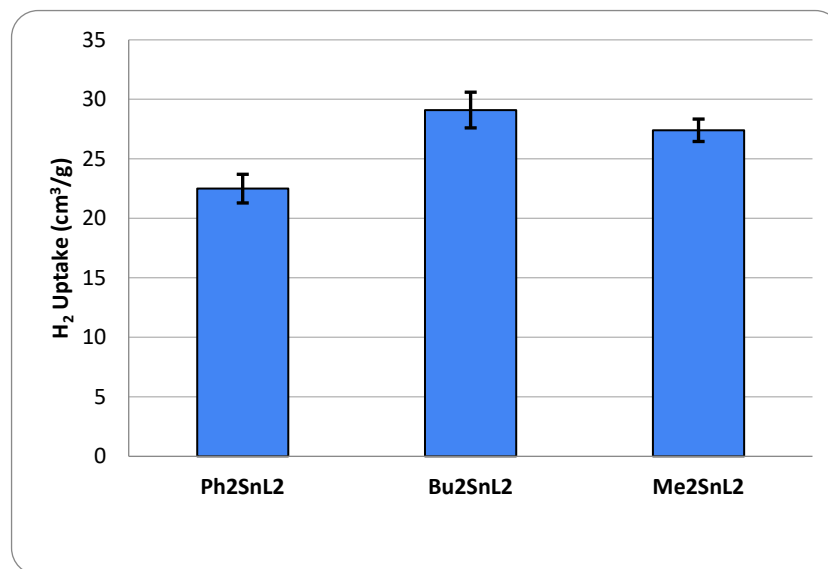


Figure 3. Hydrogen uptake for sulfamethoxazole tin complexes.

The H₂ uptake capacities of the fabricated complexes were comparable to those of polyphosphate and fusidate metal complexes used as adsorbents (Table 6). However, in the present study, high pressure is required to restrict the applicability of the fabricated materials as hydrogen storage media [33]. The mechanism for H₂ uptake in both cases involves physisorption, where hydrogen molecules interact with the surface of the complexes through weak van der Waals forces. The surface area and pore structure of the complexes influence this interaction. The L₂SnR₂ complexes exhibit similar mechanisms due to their structural similarities, as described in the manuscript.

Table 6. Hydrogen uptake capacity of various adsorbents.

Adsorbent	Hydrogen Uptake (cm ³ /g)	Condition	References
Bu ₂ SnL ₂	29.1 ± 1.46	323 K and 50 bar	Current work
Fusidate zinc complex	2.8	323 K and 50 bar	[30]
Polyphosphate	7.4	323 K and 50 bar	[34]

4. Conclusions

This study successfully synthesized and characterized novel sulfamethoxazole organotin complexes using various techniques, including NMR, FTIR spectroscopy, FESEM, and BET surface area analysis. The complexes demonstrated significant hydrogen storage capabilities, where the highest hydrogen uptake was observed at 323 K. These complexes' structural and surface characteristics, such as morphology and porosity, were found to play crucial roles in their gas adsorption properties. The sulfamethoxazole dibutyl tin complex had a surface area of 13.792 m²/g among the three prepared complexes. The gas adsorption was affected by the gas composition, the metal used within the complex, and the volume and diameter of the surface pores. The findings suggest that sulfamethoxazole organotin complexes could solve gas pollution and global warming problems by separating and storing gas. These complexes could be used in sustainable energy storage systems after further optimization and application research.

Supplementary Materials: The following supporting information can be downloaded at <https://www.mdpi.com/article/10.3390/hydrogen5040045/s1>, Figure S1: ^1H NMR spectrum of sulfamethoxazole Schiff base (L); Figure S2: ^{13}C NMR spectrum of sulfamethoxazole Schiff base (L); Figure S3: ^{119}Sn NMR spectrum of Ph_2SnL_2 complex; Figure S4: ^{119}Sn NMR spectrum of Bu_2SnL_2 complex; Figure S5: ^{119}Sn NMR spectrum of Me_2SnL_2 complex.

Author Contributions: E.Y. and D.S.A. designed the work, conducted the experiments, and wrote the first draft; N.E. and M.A.-M. characterized the materials; M.K. and M.A.-M. wrote, revised, and edited the manuscript; E.Y. supervised the work and administration. All authors have read and agreed to the published version of the manuscript.

Funding: This research received no external funding.

Data Availability Statement: Data are contained within the article.

Acknowledgments: The authors would like to thank Al-Nahrain University for giving them access to the required labs.

Conflicts of Interest: The authors declare no conflicts of interest.

References

1. Ibrahim, M.; Vo, X.V. Exploring the Relationships among Innovation, Financial Sector Development and Environmental Pollution in Selected Industrialized Countries. *J. Environ. Manag.* **2021**, *284*, 112057. [[CrossRef](#)] [[PubMed](#)]
2. Ma, X.; Wu, Y.; Fang, M.; Liu, B.; Chen, R.; Shi, R.; Wu, Q.; Zeng, Z.; Li, L. In-Situ Activated Ultramicroporous Carbon Materials Derived from Waste Biomass for carbon dioxide Capture and Benzene Adsorption. *Biomass Bioenergy* **2022**, *158*, 106353. [[CrossRef](#)]
3. Keith, D.W. Why Capture carbon dioxide from the Atmosphere? *Science* **2009**, *325*, 1654–1655. [[CrossRef](#)]
4. Bergstra, A.D.; Brunekreef, B.; Burdorf, A. The Influence of Industry-Related Air Pollution on Birth Outcomes in an Industrialized Area. *Environ. Pollut.* **2021**, *269*, 115741. [[CrossRef](#)]
5. Goh, K.; Karahan, H.E.; Yang, E.; Bae, T.-H. Graphene-Based Membranes for carbon dioxide/ CH_4 Separation: Key Challenges and Perspectives. *Appl. Sci.* **2019**, *9*, 2784. [[CrossRef](#)]
6. Sethia, G.; Sayari, A. Activated carbon with optimum pore size distribution for hydrogen storage. *Carbon* **2016**, *99*, 289–294. [[CrossRef](#)]
7. Rosi, N.L.; Eckert, J.; Eddaoudi, M.; Vodak, D.T.; Kim, J.; O’Keeffe, M.; Yaghi, O.M. Hydrogen storage in microporous metal-organic frameworks. *Science* **2003**, *300*, 1127–1129. [[CrossRef](#)]
8. Orimo, S.; Nakamori, Y.; Eliseo, J.R.; Züttel, A.; Jensen, C.M. Complex hydrides for hydrogen storage. *Chem. Rev.* **2007**, *107*, 4111–4132. [[CrossRef](#)] [[PubMed](#)]
9. Van den Berg, A.W.C.; Areán, C.O. Materials for hydrogen storage: Current research trends and perspectives. *Chem. Commun.* **2008**, *6*, 668–681. [[CrossRef](#)]
10. Unger, K. Structure of Porous Adsorbents. *Angew. Chem. Internat. Edit.* **1972**, *11*, 267–278. [[CrossRef](#)]
11. Bao, L.; Gao, P.; Peng, S. Analysis Method of Pore Size Distribution of Porous Materials. *Mater. Sci.* **2020**, *10*, 95–103.
12. Ying, J.Y.; Mehner, C.P.; Wong, M.S. Synthesis and Applications of Supramolecular-Templated Mesoporous Materials. *Angew. Chem. Int. Ed.* **1999**, *38*, 56–77. [[CrossRef](#)]
13. Yu, J.C.; Wang, X.; Fu, X. Pore-Wall Chemistry and Photocatalytic Activity of Mesoporous Titania Molecular Sieve Films. *Chem. Mater.* **2004**, *16*, 1523–1530. [[CrossRef](#)]
14. Hou, K.; Tian, B.; Li, F.; Bian, Z.; Zhao, D.; Huang, C. Highly Crystallized Mesoporous TiO_2 Films and Their Applications in Dye Sensitized Solar Cells. *J. Mater. Chem.* **2005**, *15*, 2414–2420. [[CrossRef](#)]
15. Choi, S.Y.; Mamak, M.; Coombs, N.; Chopra, N.; Ozin, G.A. Electrochromic Performance of Viologen-Modified Periodic Mesoporous Nanocrystalline anatase Electrodes. *Nano Lett.* **2004**, *4*, 1231–1235. [[CrossRef](#)]
16. Ye, B.; Trudeau, M.; Antonelli, D. Synthesis and Electronic Properties of Potassium Fulleride Nanowires in a Mesoporous Niobium Oxide Host. *Adv. Mater.* **2001**, *13*, 29–33. [[CrossRef](#)]
17. Skadtchenko, B.O.; Trudeau, M.; Kwon, C.W.; Dunn, B.; Antonelli, D. Antonelli, Synthesis and Electrochemistry of Li-and Na-Fulleride Doped Mesoporous Ta oxides. *Chem. Mater.* **2004**, *16*, 2886–2894. [[CrossRef](#)]
18. Zhe, L.Z.; Zheng, H.Y. Theoretical and Practical Discussion of Measurement Accuracy for Physisorption with Micro-and Mesoporous Materials. *Chin. J. Catal.* **2013**, *34*, 1797–1810. [[CrossRef](#)]
19. Al-Masoudi, W.; Jassim, S.; Khassaf, H. Synthesis and evolution of sulfamethoxazole derivative and assay antibacterial activity. *Basrah J. Vet. Res.* **2021**, *20*, 1–7. [[CrossRef](#)]
20. Alhaydari, E.; Yousif, E. Synthesize and Characterize Dibutyltin (IV) Oxide Complex by Utilizing New Ligand. *Al-Nahrain J. Sci.* **2021**, *24*, 1–6. [[CrossRef](#)]
21. Hussain, Z.; Yousif, E.; Ahmed, A.; Altaie, A. Synthesis and characterization of Schiff’s bases of sulfamethoxazole. *Org. Med. Chem. Lett.* **2014**, *4*, 1–4. [[CrossRef](#)] [[PubMed](#)]

22. Arraq, R.R.; Hadi, A.G.; Ahmed, D.S.; El-Hiti, G.A.; Kariuki, B.M.; Husain, A.A.; Bufaroosha, M.; Yousif, E. Enhancement of photostabilization of poly (vinyl chloride) in the presence of tin–cephalexin complexes. *Polymers* **2023**, *15*, 550. [[CrossRef](#)] [[PubMed](#)]
23. Hussein, A.K.; Yousif, E.A.; Rasheed, M.K.; Ahmed, D.S.; Bufaroosha, M.; Abdallah, M.; Al-Mashhadani, M.; Hashim, H.; Rashad, A.; Yusop, R.; et al. Application of Metal Oxides Nanoparticles to Enhance Ultraviolet Light Resistance of Polyvinyl Chloride Films. *J. Curr. Sci. Technol.* **2024**, *14*, 71. [[CrossRef](#)]
24. Watheq, B.; Yousif, E.; Al-Mashhadani, M.H.; Mohammed, A.; Ahmed, D.S.; Kadhom, M.; Jawad, A.H. A surface morphological study, poly (vinyl chloride) photo-stabilizers utilizing ibuprofen tin complexes against ultraviolet radiation. *Surfaces* **2020**, *3*, 579–593. [[CrossRef](#)]
25. Alhaydary, E.; Yousif, E.; Al-Mashhadani, M.H.; Ahmed, D.S.; Jawad, A.H.; Bufaroosha, M.; Ahmed, A.A. Sulfamethoxazole as a ligand to synthesize di- and tri-alkyltin (IV) complexes and using as excellent photo-stabilizers for PVC. *J. Polym. Res.* **2021**, *28*, 469. [[CrossRef](#)]
26. Yu, S.; Li, C.; Fan, S.; Wang, J.; Liang, L.; Hong, M. Three organotin (IV) Schiff-base carboxylates: Synthesis, structural characterization and in vitro cytotoxicity against cis-platin-resistant cancer cells. *J. Mol. Struct.* **2022**, *1257*, 132585. [[CrossRef](#)]
27. Ibraheem, H.A.; El-Hiti, G.A.; Yousif, E.; Ahmed, D.S.; Kariuki, B.M. Modified polymethyl methacrylate as a sustainable medium for capturing carbon dioxide. *Mater. Lett.* **2024**, *372*, 137031. [[CrossRef](#)]
28. Li, J.R.; Kuppler, R.J.; Zhou, H.C. Selective gas adsorption and separation in metal–organic frameworks. *Chem. Soc. Rev.* **2009**, *38*, 1477–1504. [[CrossRef](#)] [[PubMed](#)]
29. Ma, X.; Albertsma, J.; Gabriels, D.; Horst, R.; Polat, S.; Snoeks, C.; Kapteijn, F.; Eral, H.; Vermaas, D.; Mei, B.; et al. Carbon monoxide separation: Past, present and future. *Chem. Soc. Rev.* **2023**, *52*, 3741–3777. [[CrossRef](#)]
30. Hu, J.; Yang, S.; Wang, X.; Zhang, D.; Tan, B. High Pore Volume Hyper-Cross-Linked Polymers via Mixed-Solvent Knitting: A Route to Superior Hierarchical Porosity for Methane Storage and Delivery. *Macromolecules* **2024**, *57*, 5507–5519. [[CrossRef](#)]
31. Gao, Y.; Wang, Y.; Chen, X. Adsorption and Diffusion Characteristics of CO₂ and CH₄ in Anthracite Pores: Molecular Dynamics Simulation. *Processes* **2024**, *12*, 1131. [[CrossRef](#)]
32. Zhang, S.; Zhang, X.; Wang, Z.; Liu, X.; Heng, S.; Li, Y.; Sun, Z. Molecular simulation of CH₄ and CO₂ adsorption behavior in coal physicochemical structure model and its control mechanism. *Energy* **2023**, *285*, 129474. [[CrossRef](#)]
33. Juan-Juan, J.; Marco-Lozar, J.P.; Suárez-García, F.; Cazorla-Amorós, D.; Linares-Solano, A. A comparison of hydrogen storage in activated carbons and a metal–organic framework (MOF-5). *Carbon* **2010**, *48*, 2906–2909. [[CrossRef](#)]
34. Ahmed, D.S.; El-Hiti, G.A.; Yousif, E.; Hameed, A.S.; Abdalla, M. New Eco-Friendly Phosphorus Organic Polymers as Gas Storage Media. *Polymers* **2017**, *9*, 336. [[CrossRef](#)]

Disclaimer/Publisher’s Note: The statements, opinions and data contained in all publications are solely those of the individual author(s) and contributor(s) and not of MDPI and/or the editor(s). MDPI and/or the editor(s) disclaim responsibility for any injury to people or property resulting from any ideas, methods, instructions or products referred to in the content.